Acta Cryst. (1996). D52, 77–86

Structure of Flavoprotein FP_{390} from a Luminescent Bacterium *Photobacterium phosphoreum* Refined at 2.7 Å Resolution

AKIKO KITA,[a,b] SABU KASAI,[c] MAKOTO MIYATA[d] AND KUNIO MIKI[b]*

[a]*Research Laboratory of Resources Utilization, Tokyo Institute of Technology, Nagatsuta, Midori-ku, Yokohama 227, Japan,* [b]*Department of Chemistry, Faculty of Science, Kyoto University, Sakyo-ku, Kyoto 606-01, Japan,* [c]*Department of Bioapplied Chemistry, Faculty of Engineering, Osaka City University, Sugimoto, Sumiyoshi-ku, Osaka 558, Japan, and* [d]*Department of Biology, Faculty of Science, Osaka City University, Sugimoto, Sumiyoshi-ku, Osaka 558, Japan*

(*Received 17 January 1995; accepted 18 July 1995*)

Abstract

The three-dimensional structure of a flavoprotein, FP_{390}, from a luminescent bacterium, *Photobacterium phosphoreum*, solved by the molecular-replacement method, was refined to an R factor of 24.0% for 17433 independent reflections, from 6.0 to 2.7 Å resolution, collected by synchrotron radiation. The asymmetric unit of the crystal (space group $P4_322$, $a = b = 76.8$ and $c = 242$ Å) contains two monomer molecules related by a non-crystallographic twofold axis to form a dimer. There are two Q-flavin [flavin mononucleotide (FMN) with myristic acid] molecules in FP_{390} monomer. One of them is located at the interface of dimer which is bound to both monomer and the another is at the molecular surface. The electron density of myristic acids of Q-flavins at the dimer interface in both monomer are weak and unclear, showing the possibility that the Q-flavins bound in this site are not a single species but a mixture of two components, 6-(3″-myristic acid)–FMN and 6-(4″-myristic acid)–FMN.

1. Introduction

Bioluminescent organisms are widely seen in nature and comprise a remarkably diverse set of species. The bacterial luciferase has been studied most intensively in these organisms from a variety of viewpoints (Hastings, Potrikus, Gupta, Kurfurst & Makemson, 1985; Meighen, 1991; Baldwin & Ziegler, 1992). The *in vitro* light-emitting reaction scheme has been established as,

$$\mathrm{FMNH_2} + \mathrm{O_2} + R\mathrm{CHO} \rightarrow R\mathrm{COOH} + \mathrm{FMN} + \mathrm{H_2O} + h\nu.$$

However, it is questionable whether the same reaction actually proceeds in living cells. It was proposed that the physiological function of bacterial luciferase would not be to produce light but to produce P-flavin, which is a flavin compound bound to luciferase (Kasai, 1994).

A yellow protein named flavoprotein 390 (FP_{390}), because of its absorption maximum at 390 nm, was found during the purification step of luciferase of *Photobacterium phosphoreum* (Kasai, Matsui & Nakamura, 1987). Because biosynthesis of FP_{390} is induced under the same conditions in which luciferase is induced, it was inferred that a gene coding for FP_{390} should be included in the *lux* operon, which contains genes related to the bacterial bioluminescence. Thereafter, a new gene was found only in the *lux* operon of *Photobacterium* species. These genes were designated as *luxF* (Mancini, Boylan, Soly, Graham & Meighen, 1988) in *P. phosphoreum* and *luxG* (Illarionov, Protopopova, Karginov, Mertvetsov & Gitelson, 1988) or *luxABN* (Baldwin, Devine, Henckel, Lin & Shadel, 1989) in *P. leiognathi*, and the nucleotide sequences of both genes were determined (Soly, Mancini, Ferri, Boylan & Meighen, 1988; Illarionov *et al.*, 1988; Baldwin *et al.*, 1989). It was concluded that FP_{390} is identical to luxF protein; *i.e.*, the *luxF* gene codes for FP_{390}, by means of comparison between FP_{390} and luxF proteins by the molecular weight, the amino-acid composition of each entire protein, of all five CNBr fragments and the partial amino-acid sequences of three large CNBr fragments (Kasai *et al.*, 1991). Consequently, FP_{390} is expected to be composed of 231 amino-acid residues and its molecular weight is estimated at 26800 Da. On the other hand, the protein coded by *luxG* or *luxABN* has been called non-fluorescent flavoprotein (NFP). The crystal structure of NFP from *P. leiognathi* was determined by Moore, James, O'Kane & Lee (1992, 1993). FP_{390} also possesses substantial amino-acid sequence identity with α- and β-subunits of bacterial luciferase. Especially the β-subunit which has a 29% homology with FP_{390} when their sequences are aligned (Soly *et al.*, 1988).

The physiological function of FP_{390} is still unclear. However, it is known that FP_{390} contains a modified flavin prosthetic group, Q-flavin (Kasai *et al.*, 1991), which consists of flavin mononucleotide (FMN) and myristic acid and seems to be the same compound as a luciferase prosthetic group, P-flavin. It is curious that

Q-flavin is always released from the apoFP_{390} as a mixture of two components; the major component has been named QF_1, while the minor one has been named QF_2 (Kasai *et al.*, 1991). The structure of QF_1 and QF_2 were determined to be 6-(3″-myristic acid)-FMN and 6-(4″-myristic acid), respectively (Fig. 1). This fact may imply that two different types of flavin molecules are accommodated in a protein molecule of FP_{390}. The idea that this might be related to the function of FP_{390} turned our attention to its molecular structure. We have determined the crystal structure of FP_{390} at 3 Å resolution to obtain information about its function from the structural point of view (Kita, Kasai & Miki, 1995). The structure showed that there are two flavin binding sites in an FP_{390} molecule, but the resolution limit of the crystals did not allow us to discuss the structure of the molecules accommodated in each binding site.

We have remeasured the diffraction intensities to obtain the data as high as possible in its quality and resolution, although the crystals have a point where the diffraction intensities are suddenly weakened. We report here the three-dimensional structure of FP_{390} refined at 2.7 Å resolution based on the diffraction data remeasured by synchrotron radiation.

2. Experimental procedure

2.1. *Nucleotide sequencing of the luxF gene of P. phosporeum*

The nucleotide sequence of the *luxF* gene of the present strain of *P. phosphoreum* was determined to reconfirm the amino-acid sequence of FP_{390}. Genomic DNA was prepared from *P. phosphoreum* (IFO 13896) according to the manual of Sambrook, Fritsch & Maniatis (1989). The *luxF* gene region, expanding from the 3′ terminus of the *luxB* gene to the 5′ terminus of the *luxE* gene, was divided into three fragments designated as Fr-1, Fr-2 and Fr-3 as shown in Fig. 2. These three DNA fragments were amplified by the polymerase chain reaction (PCR) using the prepared genomic DNA as a template. Three sets of primers for Fr-1 to Fr-3 were designed by referring to the sequence reported by Soly *et al.* (1988) and Soly & Meighen (1991) as follows; 5′-AAAGAATTTACCAAGCTCCGT-3′ and 5′-GCT-GCAATATCAACTGTGTT-3′, 5′-TATGTGCTTGTCA-CCAGTA-3′ and 5′-TCTTTATAACTCCCTGTCAC-3′, and 5′-GATAGTATTATTCAGAGTAA-3′ and 5′-GTA-TCTAATGTAATAGTCAT-3′, respectively. These primers were purchased from Biosynthesis, Lewisvills, TX. Each fragment amplified by PCR was purified using gel electrophoresis, ligated into pGEM-T (Promega), and cloned in *E. coli* XL1-Blue. Nucleotide sequencing was carried out by the dideoxy method using *Bca*BEST Dideoxy Sequencing Kit (Takara) and ALF DNA Sequencer (Pharmacia Biotech). Three independently amplified clones for each fragment were sequenced for both strands.

2.2. *Crystallization and data collection*

FP_{390} was isolated from a brightly luminescent strain of *P. phosphorous* (IFO 13896). The purification and crystallization procedure have been described previously (Kasai *et al.*, 1987; Kita, Kasai, Kasai, Nakaya & Miki, 1991). Crystals were grown using potassium phosphate as a precipitating agent. Protein solution of concentrations 200–250 mg ml^{-1} and 1.6–2.2 *M* potassium phosphate at pH 9.0 were vapor equilibrated at 293 K to outer solutions with precipitant concentration of 1.8–2.5 *M* (Kita *et al.*, 1991).

X-ray intensity data were collected with synchrotron radiation at 2.5 GeV at the BL6A beamline of the Photon Factory, the National Laboratory for High Energy Physics, Japan. Two crystals were mounted in glass capillaries with a trace amount of the mother liquor so as to orient the a^* and c^* axes along the spindle axis. The X-ray beam was monochromatized to 1.00 Å by Si^{111} monochromator system. A screenless Sakabe Weissenberg camera with a cylindrical cassette of radius 430 mm was used (Sakabe, 1991). Diffraction intensities were recorded on a 200 × 400 mm imaging plate (Fuji Photo Film Co. Ltd) (Miyahara, Takahashi, Amemiya,

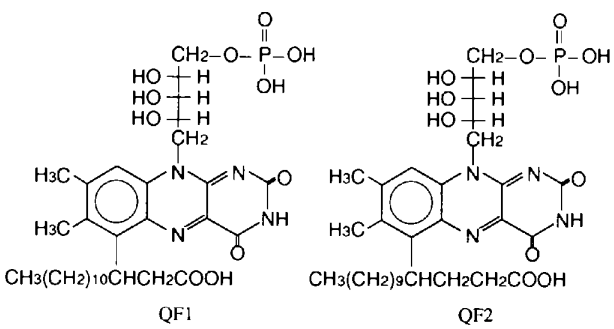

Fig. 1. QF_1, 6-(3″-myristic acid)–FMN and QF_2, 6-(4″-myristic acid)–FMN.

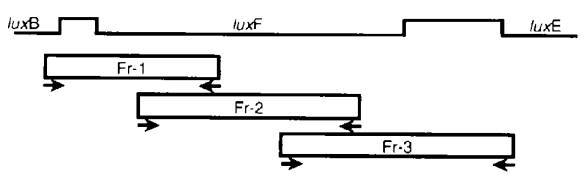

Fig. 2. The location of the three genes in the *lux* operon and three DNA fragments. The map of DNA shows the location of the three *lux* genes, *B*, *F* and *E*. Three boxes represent DNA fragments, Fr-1, Fr-2 and Fr-3, amplified using PCR and the small arrows under the boxes indicate the primers for PCR.

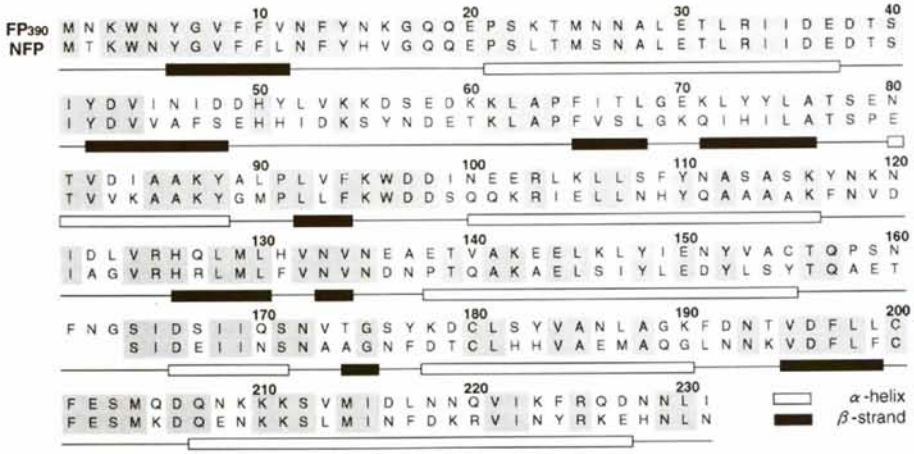

Fig. 3. An alignment of amino-acid sequences of FP_{390} and NFP (Illarionov *et al.*, 1988) and the secondary-structure assignments (Kabsch & Sander, 1983) of FP_{390} (based on monomer 1). Common residues are indicated by a gray background and α-helixes and β-strands are indicated as □ and ■, respectively.

Kamiya & Satow, 1986) using 21 and 16 sheets for rotation settings of the a^* and c^* axes, respectively. The plates were digitized at 100 μm intervals on a Fujix BA100 read-out system (Fuji Photo Film Co. Ltd). The intensity data were processed using the *WEIS* program system (Higashi, 1989) on a FACOM M780/10 computer. After the intensities of individual plates were scaled and combined within each crystal, two native data from each crystal with the different rotation axis were merged by the *PROTEIN* program system (Steigemann, 1992). The details of data collection and processing are given in Table 1. In spite of repeated data collections, the diffraction data higher than 2.7 Å resolution were not significantly measured and could not be employed for the further structure analysis. The V_m value of FP_{390} (3.3 $Å^3$ Da^{-1}) (Matthews, 1968) is much larger than that of NFP (2.4 $Å^3$ Da^{-1}) (Moore *et al.*, 1992), showing a higher solvent content in the FP_{390} crystals. This affects the present resolution limit of the FP_{390} crystals compared with the NFP crystals (2.2 Å resolution) (Moore *et al.*, 1992).

3. Structure solution and refinements

3.1. *Molecular replacement*

The crystal structure of FP_{390} was solved by the molecular-replacement procedure using the molecular model of NFP from *P. leiognathi* (Moore *et al.*, 1993) as previously reported (Kita *et al.*, 1995). A Patterson-search technique (Rossmann & Blow, 1962; Huber, 1965) was used on the basis of the molecular model excluding two molecules of the flavin cofactors. Cross-rotation functions were calculated using *PROTEIN* (Steigemann, 1992). An NFP molecule in an asymmetric unit forms a dimer by a crystallographic twofold axis in the NFP crystal (Moore *et al.*, 1993), whereas two crystallographically independent molecules exist in an

(*a*)

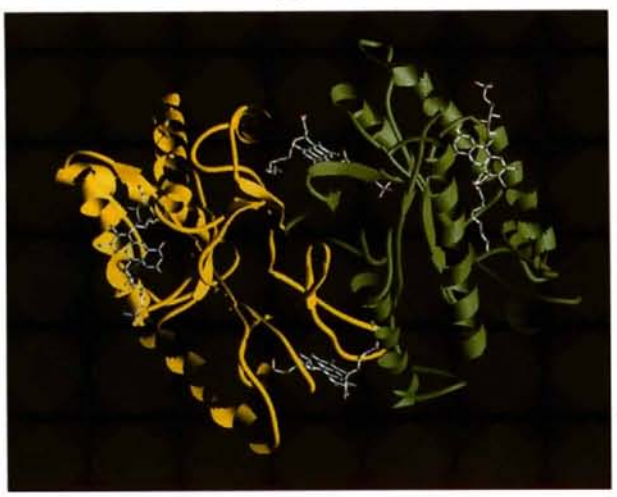

(*b*)

Fig. 4. A schematic view of the FP_{390} dimer drawn by *Ribbons* (Carson, 1991). Monomer 1 is drawn in yellow and monomer 2 in green. (*a*) A view nearly perpendicular to the local twofold axis. (*b*) A view nearly along the local twofold axis.

Table 1. *Summary of intensity data collection and processing*

Crystal data	Space group $P4_122$		
	Unit-cell dimensions	$a = b$ (Å)	76.8
		c (Å)	242
Crystal		I	II
Crystal size (mm)		1.5 × 1.5 × 0.3	0.8 × 0.8 × 0.15
Spindle axis		a^*	c^*
Collimator size (mm)		0.2	0.1
Total exposure time (s)		1672	2112
Total rotation angle (°)		105.75	48.3
No. of imaging plates		21	16
No. of reflections (6.0–2.7 Å)			
measured		79128	34307
independent		16286	12572
R_{merge} between plates*		0.080	0.065
Completeness of reflections (%)			
6.00–2.70 Å		86.9	67.1
2.76–2.70 Å		70.0	38.8

Merged I and II

No. of independent reflections	17448
R_{merge} between crystals*	0.062
Completeness of reflections (%)	
6.00–2.70 Å	93.1
2.76–2.70 Å	81.9

* The merging R factor is defined as $\sum |I_i - \langle I \rangle| / \sum I$, where I_i is an individual intensity measurement and $\langle I \rangle$ is the average intensity for this reflection.

Table 2. *Summary of refinement statistics*

Resolution range (Å)	6.00–2.70
No. of protein atoms	3748
No. of cofactor atoms	188
No. of water molecules	62
No. of reflections	17433
R factor (%)	24.0

R.m.s. deviations of geometry from ideal values (target σ)

Distances	
Bond (Å)	0.010 (0.020)
Angle (Å)	0.033 (0.035)
Planar (Å)	0.038 (0.050)
Planar groups (Å)	0.008 (0.020)
Chiral volumes (Å^3)	0.146 (0.150)
Non-bonded contacts	
Single torsion (Å)	0.211 (0.300)
Multiple torsion (Å)	0.253 (0.300)
Possible hydrogen-bond (Å)	0.248 (0.300)
Torsion angles	
Peptide plane (°)	1.4 (3.0)
Staggered (°)	23.5 (15.0)
Transverse (°)	30.1 (20.0)

asymmetric unit to form a dimer in the present FP_{390} crystal. The both monomeric and dimeric models were placed in a cubic cell with a side length of 200 Å, with the center of gravity at the origin. Triclinic structure factors were then calculated in the resolution range from 6.0 to 3.5 Å. After Patterson functions were calculated, 8234 and 9224 highest peaks with the range of vector lengths from 10 to 50 Å were selected from the Patterson maps of the monomeric and dimeric models, respectively. The correlation functions between the FP_{390} crystal and the model Patterson function were calculated in steps of 5°, and subsequently in steps of 1° around high correlation peaks. Clear maximum peaks appeared in both cases using the monomeric and dimeric model at ψ (inclination against y) = 81.9°, φ (azimuth relative to x) = 88.9° and κ (rotating angle around z) = 45.3°, and ψ = 80.3°, φ = 91.4° and κ = 43.3°, respectively. The models were rotated and applied for calculation of the translation function.

The location of correctly oriented molecules were determined by the translation function of Crowther & Blow (1967) using the program written by E. E. Lattmann. The model Fourier transforms were calculated for the orthogonal cell axis of 150 Å using data from 10.0 to 4.0 Å resolution. The translation function was determined in steps of 1 Å. Prominent peaks were given only when the dimeric model was used. Most of peaks on Harker sections were more than ten times the standard deviations. The vector set generated from molecules at the equivalent positions at (x, y, z) and $(y, -x, z + \frac{3}{4})$ was searched in the Harker sections of $w = \frac{1}{4}$ and $w = \frac{3}{4}$. The highest peak (about 10σ) was found at $w = \frac{3}{4}$, whereas there was only a minor peak at $w = \frac{1}{4}$. This indicated that the correct space group is $P4_122$ instead of $P4_122$. The final positions of center of gravity of dimer model were $x = 9.4$, $y = 37.7$ and $z = 89.7$ Å.

3.2. *Model building and crystallographic refinement*

The protein model obtained by molecular replacement was initially refined by the *X-PLOR* program (Brünger, 1992) using the data from 6.0 and 3.0 Å resolution. Rigid-body minimization taking each monomer as a rigid body where the Q-flavin model contains no myristic acids reduced the R factor to 4.08%. At this stage, the amino-acid residues in the model were correctly replaced by those of FP_{390}. The R factor decreased to 29.7% after the conventional energy-restrained positional refinement. The subsequent simulated-annealing refinement with the fixed overall B factor of 15 Å^2 converged the R factor to 20.5%. Hereafter, myristic acids were added to the flavin model so as to fit the omit maps with coefficients $2F_o - F_c$ and $F_o - F_c$. All the model building and adjustments were performed on an Evans and Sutherland interactive display system using the program *FRODO* (Jones, 1978). Further crystallographic refinement was performed by the stereochemically restrained least-squares method using the *CONEXN/PROTIN/PROLSQ* program package (Hendrickson, 1985; Pähler & Hendrickson, 1990), where the data were expanded to the resolution range between 6.0 and 2.7 Å with $2\sigma(F)$ cut-off. Individual isotropic temperature factors were

introduced and 61 water molecules selected from peaks which appeared in both $2F_o - F_c$ and $F_o - F_c$ electron-density maps were added to the model. The final R factor is 24.0% for the data from 6.0 to 2.7 Å resolution. The mean temperature factor of non-H atoms of the apoFP_{390} (3748 atoms in total) is 34.5 Å^2. R.m.s. deviations from the ideal values were 0.010 Å for bond lengths and 2.3° for bond angles. The mean positional error of atoms estimated from a Luzzati plot (Luzzati, 1952) is 0.40 Å. The refinement statistics are summarized in Table 2.

All calculations for the molecular replacement and refinement were carried out on a VAXstation 4000/90 computer.

4. Results and discussion

4.1. *Nucleotide sequence of luxF gene of P. phosphoreum (IFO 13896) and deduced amino-acid sequence of FP_{390}*

The determined nucleotide sequences from *P. Phosphoreum* IFO 13896 were compared with that from NCMB 844 reported by Soly *et al.* (1988) and Soly & Meighen (1991). The DNA sequence of *luxF* gene and flanking non-coding region from two strains were identical with one exception; the 190th nucleotide from the beginning of the *luxF* gene was reported to be T in NCMB 844 whereas C was found in IFO 13896. However, T might be reported erroneously in NCMB 844 because the corresponding nucleotide in the *luxF* [designated as *luxG* by Illarionov *et al.* (1988) or *luxABN* by Baldwin *et al.* (1989)] gene from *P. leiognathi* was reported to be C. Although the 64th amino-acid residue of FP_{390} is deduced to be Ser in NCMB 844, this residue is deduced to be Pro in IFO 13896 as in *P. leiognathi* (Illarionov *et al.*, 1988; Baldwin *et al.*, 1989). A mutation of Pro to Ser or its inverse seems to occur infrequently, as replacement of Pro residues for other amino-acid residues often causes a drastic structural change in the protein. However, the strain IFO 13896 either seems to be identical with the strain NCMB 844 or derived from this strain. IFO 13896 seems to have been isolated originally from the epidermis of squid and identified as *P. phosphoreum* at the Institute for Fermentation, Osaka by Imai (1981) and given an IFO number. It is unclear why the strain identical with NCMB 844 was isolated from a Japanese squid. The alignment of the amino-acid sequences of FP_{390} and NFP (Illarionov *et al.*, 1988) is presented in Fig. 3.

4.2. *Dimer structure of FP_{390}*

The structure of the FP_{390} dimer molecule is presented in Fig. 4. The chain folding of each monomer is similar to the three-dimensional structure of NFP which has 55% amino-acid sequence identity (Moore *et al.*, 1993). However, each monomer molecule in the FP_{390} dimer is crystallographically independent, whereas the monomer is related by a crystallographic twofold axis to form a symmetrical homodimer in NFP (Moore *et al.*, 1993). The superposition of the Cα atoms between FP_{390} and NFP is shown in Fig. 5. The r.m.s. deviations of two FP_{390} monomers from the NFP molecule in main-chain atoms excluding the insertion region are 1.072 Å (monomer 1) and 1.074 Å (monomer 2), respectively.

Fig. 6 shows the environments of two FP_{390} monomers, which are different from each other because of the crystal packing. Monomer 1 is in rigid contact with the other four molecules from three directions, while monomer 2 is in much less contact with the other three molecules. This difference in the crystal packing seems to be related to the difference in the quality of electron densities of two monomers. In general, the electron density of monomer 1 was readily interpreted in the model rebuilding. On the other hand, that of monomer 2 was somewhat unclear and there are many regions where the model construction is more difficult than that of monomer 1. Fig. 7 shows the isotropic temperature factors of Cα atoms of the 231 amino-acid residues in the two monomers. A few regions where B factors of monomer 2 are significantly higher than those of monomer 1 have intermolecular atomic contacts with

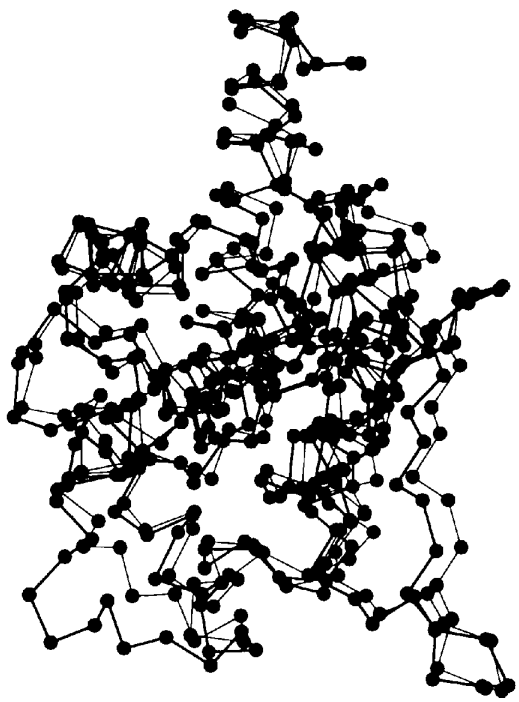

Fig. 5. The superposition of Cα atoms between FP_{390} (monomer 1) and NFP (Moore *et al.*, 1993) depicted by *MOLSCRIPT* (Kraulis, 1991). The thick line indicates the FP_{390} molecule and thin line the NFP molecule. Spheres stand for Cα atoms.

neighbouring molecules only in monomer 1. The r.m.s. deviation of main-chain atoms between the two monomers is 1.13 Å. Both monomers are related by a local dyad symmetry. In an orthogonal coordinate system the rotation matrix of main chains between the two monomers is,

$$\begin{matrix} -0.1007 & 0.9910 & -0.0880 \\ 0.9912 & 0.0923 & -0.0950, \\ -0.0861 & -0.0968 & -0.9916 \end{matrix}$$

and the translation vector (−18.50, 33.04 and 184.70 Å) translates monomer 2 into monomer 1.

(*a*)

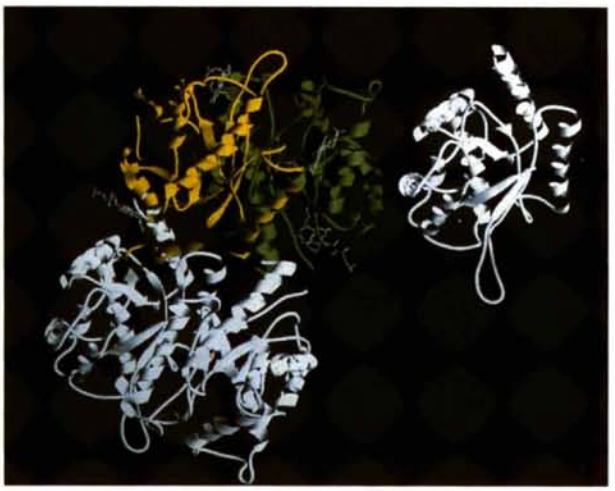

(*b*)

Fig. 6. Intermolecular contacts of each monomer of FP_{390}. Monomer 1 is presented in yellow while monomer 2 is in green, drawn by *Ribbons* (Carson, 1991). Symmetry-operated neighbor molecules whose atomic contacts are less than 4 Å are shown in white around (*a*) monomer 1 in yellow and (*b*) monomer 2 in green.

The secondary structures of FP_{390}, which are highly homologous to that of NFP (Moore *et al.*, 1993), are shown together with the amino-acid sequence in Fig. 3 and depicted schematically in Fig. 8. There are nine stranded β-sheets which form a half of the β-barrel structure and seven α-helices which surround one side of the β-barrel. In addition, a loop region like an anchor between two β-strands, *b*2 and *b*3, which are identified as pre-β strands, β2A and β2B in NFP (Moore *et al.*, 1993), protrudes to the another monomer molecule. Out of 231 amino-acid residues, there is an insertion with three amino acids in FP_{390} (residues 161–163). These residues, which connect with *a*4 and *a*5 to form a helix–loop–helix motif, are located on the molecular surface apart from the cofactor binding site. The $2F_o - F_c$ electron-density map of this loop region was unclear, especially in monomer 2, with high atomic temperature factors. Another two loop regions (residues 16–21 and 55–65) on the molecular surface near the cofactor binding pockets also have weak electron densities.

4.3. *Structures and environments of cofactors*

Two Q-flavins are accommodated in the two binding sites of an FP_{390} monomer molecule. Atomic numbering of the Q-flavin is presented in Fig. 9. One of the Q-flavins binds at the interface of dimer (QF_i) and the another at the molecular surface (QF_s), as shown in Fig. 4. The amino-acid residues used to form the QF_i binding site are essentially the same as those of NFP. Within 4 Å from the FMN moiety of QF_i, there are only two residues which are different to those of NFP; Thr60 and Lys84 in NFP are replaced with Lys and Ile, respectively. Lys84 in NFP forms a hydrogen bond with a ribityl hydroxyl group of FMN (Moore *et al.*, 1993). Although the wall for the QF_i binding site in each monomer is composed of the same amino-acid residues, the interactions between the QF_i molecule and the apoprotein are slightly different in each binding site. These interactions of the QF_i binding sites in monomers 1 and 2 are depicted in Fig. 10. The isoalloxazine ring of QF_i is stacked by Tyr14 of the another monomer from the *si*-side of the ring in each monomer. This tyrosine is conserved in the luciferase β subunit. In the α subunit of luciferase, this Tyr residue is substituted to phenylalanine which is conserved in luciferase α subunits from many species.

The electron densities of the Q-flavins at both binding sites are very weak and unclear in each monomer. The *B* factors of the Q-flavin molecules are very high, the average values of QF_i and QF_s being 43.8 and 63.9 $Å^2$, respectively. Myristic acids of QF_i are located almost perpendicular to the plane of the isoalloxazine ring. However, in both monomers, weak electron densities corresponding to those of the fatty acid moiety of myristic acid appeared discretely in both *re*- and *si*-sides of the QF_i isoalloxazine ring. Fig. 11(*a*) shows the

electron densities of QF_i in the case of monomer 2, where both models with different orientations of myristic acid chains are tentatively located. The present model is adopted so as to take the same orientation of the myristic acid chain as NFP. In this model, the side chain of Lys87 in the QF_i binding site seems to take different orientations in the two monomers. Judging from the present electron densities, this side chain is located out of the Q-flavin pocket and Lys87(Nζ) is hydrogen bonded to the water molecule in monomer 1, while Lys87(Nζ) is oriented toward the myristic acid but not hydrogen bonded to the carboxyl O atom of myristic acid in monomer 2. In NFP, both Tyr88(Oη) and Lys87(Nζ) are hydrogen bonded to two carboxyl O atoms of myristic acid (Moore *et al.*, 1993). The possibility that myristic acid has the opposite orientation cannot be excluded for the present electron densities, which implies a type of disorder involving two opposite orientations of the myristic acid chain. However, both Tyr88 and Lys87 in NFP mentioned above are conversed in FP_{390}. If myristic acid of QF_i in FP_{390} takes an opposite orientation to that of NFP, the carboxyl groups are free from any hydrogen bonds, which is unlikely and seems to be unfavorable.

In both monomers, the QF_s myristic acids could be located in the electron densities of the $F_o - F_c$ omit map, although the average B factor of QF_2 is larger than that of QF_1. The electron densities of the FMN moiety which is exposed to solvent area are more unclear than that of the myristic acid moiety which is accommodated into the inner part of the binding site. Fig. 11(*b*) shows the electron densities of QF_s in monomer 1. The ambiguity found in the case of the QF_i binding site did not occur in positioning the myristic moiety of the Q-flavin. The orientation of myristic acid takes unambiguously a similar direction to that of NFP. The electron densities of the FMN ribityl group of QF_s are too weak to determine its position without ambiguity in monomer 2. The intramolecular interactions of the QF_s binding sites for monomer 1 are depicted in Fig 12. The O2 atom in the isoalloxazine ring of QF_s is hydrogen bonded to Asn2(O). The carboxyl O atom is hydrogen bonded to Gln220(Nε) and the aliphatic chain of myristic acid is stabilized in the hydrophobic pocket. The carboxyl O atoms are located at the *re*-side of the isoalloxazine plane and the aliphatic chain at the *si*-side stretches toward the protein interior.

4.4. *The roles of two flavin binding sites*

It is curious that both QF_1 and QF_2 (Fig. 1) are always released from the FP_{390} protein as a mixture. As QF_1 and QF_2 are major and minor components, respectively, QF_2 might be a by-product in the step of Q-flavin production. Although the function of FP_{390} is unknown, if FP_{390} plays a role in some enzymatic reaction, its cofactor should not be a mixture of two components but a single compound to enable such a reaction to proceed efficiently. However, the formation of substantial amounts of by-product seems to be unavoidable in the reaction catalyzed by the bacterial luciferase because the reaction is so complicated. We have assumed that one of two Q-flavin binding sites in FP_{390} may accommodate such a by-product to avoid the formation of FP_{390} binding the by-product at the active site (Kita *et al.*, 1995). Of the two Q-flavin binding sites, one is located inside at the dimer interface and another is outside at the molecular surface. Judging from the positions of both binding sites in the protein molecule, the former seemed to be an active site and the latter was apparently a by-product binding pocket. If this is correct, the QF_i binding site would accommodate QF_1 whereas QF_s would accommodate QF_2, respectively. However, the present interpretation of electron densities showed that the QF_s binding site accommodates only the QF_1 molecules. On the other hand, the ambiguity in flavin binding lies on the QF_i binding site, where two possibilities for Q-flavin

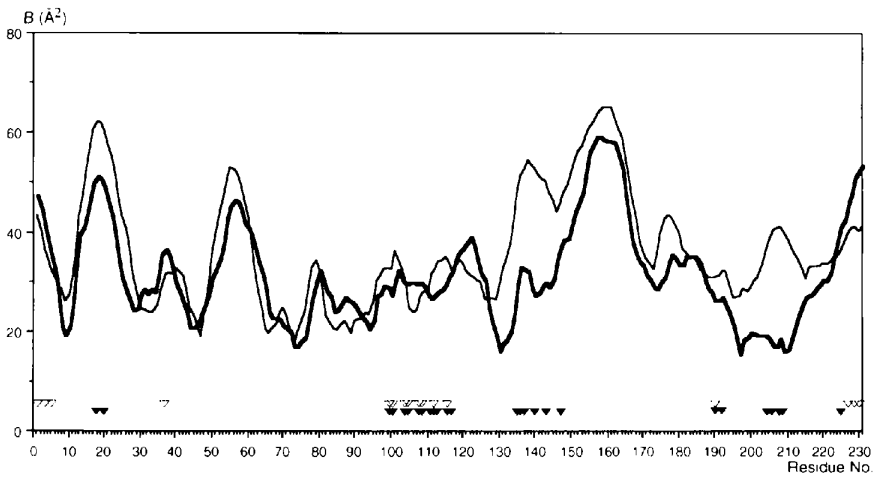

Fig. 7. A plot of the isotropic temperature factors of Cα atom of each monomer in FP_{390}. The thick line indicates monomer 1 and the thin line monomer 2. An inverted triangle indicates a residue which has intermolecular atomic contacts less than 4 Å with the other neighbor molecules operated by crystallographic symmetries (▼, monomer 1 and ▽, monomer 2).

binding are considered. (1) Both QF_1 and QF_2 are accommodated as a mixture in the same manner of the orientation of myristic acid as NFP; (2) QF_1 is accommodated in the same manner as NFP and at the same time QF_2 is bound to this pocket, although unlikely, with the opposite orientation of myristic acid for the *re*- and *si*-sides of the isoalloxazine ring. The observation that the orientation of the Lys87 side chain in QF_i seems to be different from that in NFP may support the possibility that both QF_1 and QF_2 are accommodated as a mixture in the QF_i binding site. Moreover, the active flavin binding site is located on the molecular surface in crystal structures of flavodoxin (Bernett *et al.*, 1974; Watenpaugh, Sieker & Jensen, 1973; Smith *et al.*, 1983; Fukuyama, Wakabayashi, Matsubara & Rogers, 1990), which is similar to the QF_s binding site found in FP_{390}. It seems to be difficult to solve this problem from the present quality of electron density, or even from that of higher quality because it requires the ability to distinguish the difference between molecular models of QF_1 and QF_2. The biochemical and molecular biological approaches to elucidate the function of FP_{390} should be combined with the present structural study to understand the structure–function relationship of this protein.

We would like to thank Drs S. A. Moore and M. N. G. James, University of Alberta, for their kindness in supplying us the atomic coordinates of NFP prior to deposition with the Protein Data Bank. We are also indebted to Dr M. Yoshida, Tokyo Institute of Technology, for his support and interest, and to Dr E. A. Meighen, McGill University, for his suggestion on determination of nucleotide sequence. Thanks are also due to Drs N. Sakabe, A. Nakagawa, N. Watanabe and S. Ikemizu of Photon Factory, National Laboratory for High Energy Physics, for their kind help in intensity data

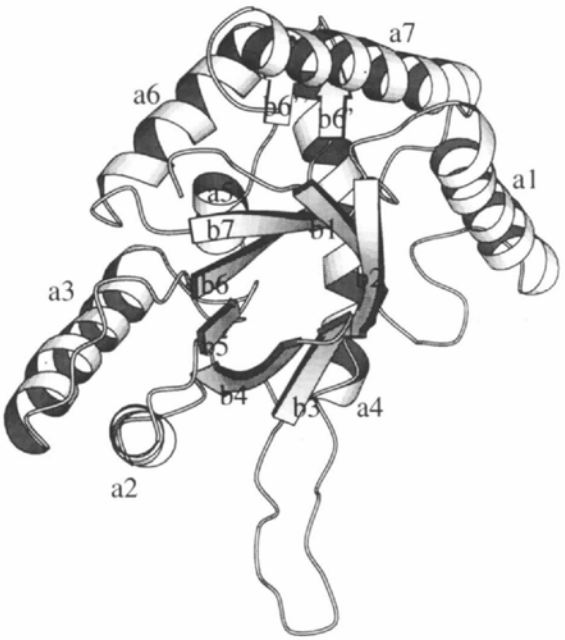

Fig. 8. Schematic representation of secondary structure of FP_{390} monomer drawn by *MOLSCRIPT* (Kraulis, 1991). The labels *a*1 to *a*7 and *b*1 to *b*7 show α-helices and β-strands in order from the N to C terminals.

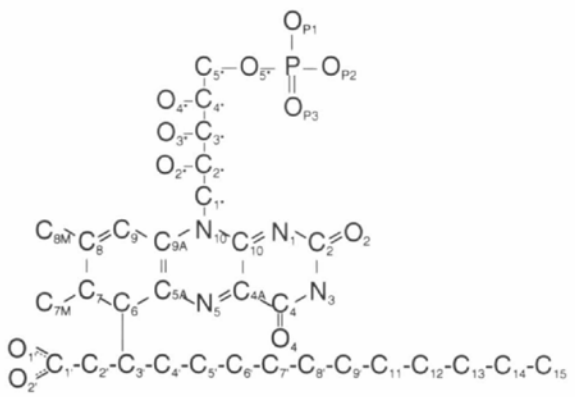

Fig. 9. The atomic numbering of Q-flavin.

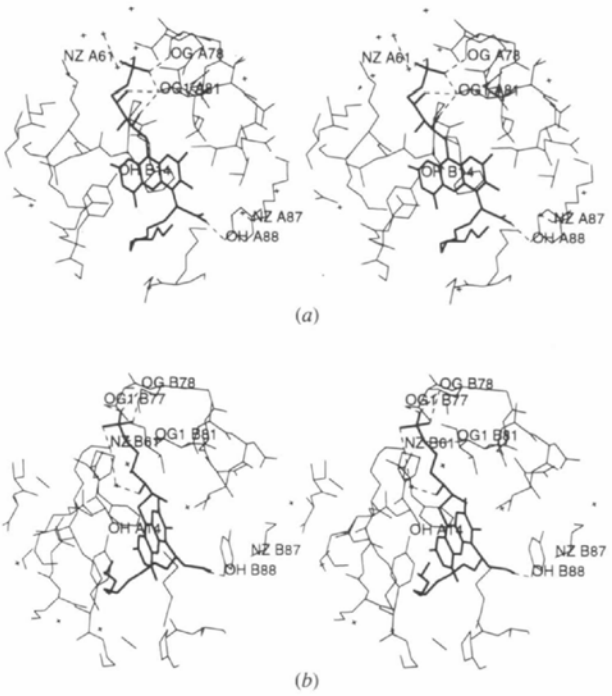

Fig. 10. Intermolecular interactions in the QF_i binding sites. (*a*) the monomer 1: hydrogen bonds are O(P1)···Ser78(Oγ), O(P1)···Thr81(Oγ1), O(P3)···WAT, O(2*)···Thr81(Oγ1), O(4*)···Thr81(Oγ1), Lys87(Nζ)···WAT, O(1')···Tyr88(Oη). (*b*) the monomer 2: O(P2)···Thr77(Oγ1), O(P2)···Ser78(Oγ), O(P1)···Ser78(Oγ), O(P3)···Lys61–N(ζ), O(5*)···Thr81(Oγ1), O(3*)···WAT, O(1')···Tyr88(η).

collection and processing, which were performed under the approval of the Photon Factory Advisory Committee (Proposal No. 90-183). This work was partly supported by Grants-in-Aid for Scientific Research on Priority Areas (No. 05244102) and for General Scientific Research (No. 06453219) to KM and also by a Grant-in-Aid for JSPS Fellows (No. 042176) to AK from the Ministry of Education, Science and Culture, Japan.*

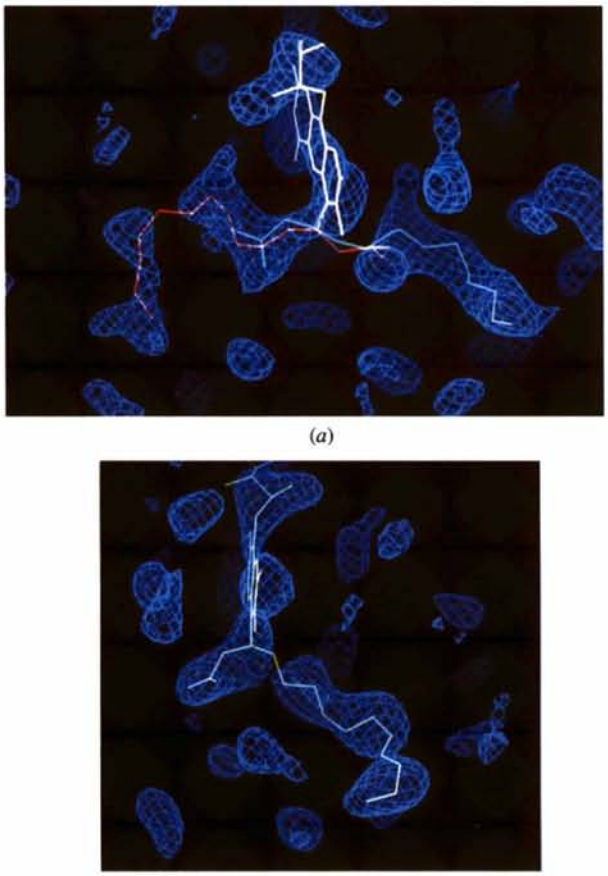

Fig. 11. Electron-density maps of myristic acid in (*a*) QF_f and (*b*) QF_s binding sites. The flavin molecule is omitted from the phase calculation. Maps were drawn at 2.0σ and 2.5σ cut-off for (*a*) and (*b*), respectively. Two types of the models for myristic acid are superimposed in light green (similar orientation to that of NFP) and in red (an opposite orientation to that of NFP).

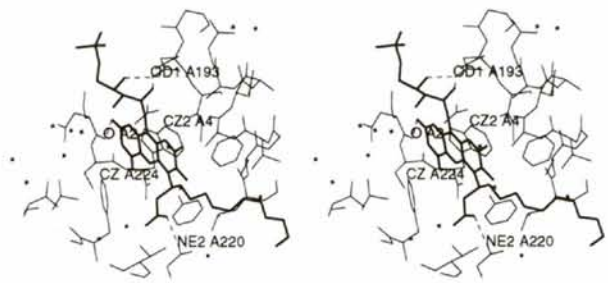

Fig. 12. Intermolecular interactions in the QF_s binding sites in monomer 1. Hydrogen bonds: O(4*)···Asn193(Oδ1), O(2*)···Asn193(Oδ1), O(2)···Asn2(O) and O(1′)···Gln220(Nε2).

* Atomic coordinates and structure factors have been deposited with the Protein Data Bank, Brookhaven National Laboratory (Reference: 1FVP, R1FVPSF). Free copies may be obtained through The Managing Editor, International Union of Crystallography, 5 Abbey Square, Chester CH1 2HU, England (Reference: AS0685).

References

Baldwin, T. O., Devine, J. H., Henckel, R. C., Lin, J. W. & Shadel, G. S. (1989). *J. Biolumin. Chemilumin.* **4**, 326–341.

Baldwin, T. O. & Ziegler, M. M. (1992). *Chemistry and Biochemistry of Flavoenzymes*, Vol. III, pp. 467–530. Boca Raton, Florida: CRC Press.

Bernett, R. M., Darling, G. D., Kendall, D. S., LeQuesne, M. E., Mayhew, S. G., Smith, W. W. & Ludwig, M. L. (1974). *J. Biol. Chem.* **249**, 4383–4392.

Brünger, A. T. (1992). *X-PLOR Version* 3.1 *Manual*. Yale University, New Haven, CT, USA.

Carson, M. (1991). *J. Appl. Cryst.* **24**, 958–961.

Crowther, R. A. & Blow, D. M. (1967). *Acta Cryst.* **23**, 544–548.

Fukuyama, K., Wakabayashi, S., Matsubara, H. & Rogers, L. J. (1990). *J. Biol. Chem.* **265**, 15804–15812.

Hastings, J. W., Potrikus, C. J., Gupta, S. C., Kurfurst, M. & Makemson, J. C. (1985). *Advances in Microbial Physiology*, pp. 235–291. London: Academic Press.

Hendrickson, W. A. (1985). *Methods Enzymol.* **115**, 252–270.

Higashi, T. (1989). *J. Appl. Cryst.* **22**, 9–18.

Huber, R. (1965). *Acta Cryst.* **19**, 353–356.

Illarionov, B. A., Protopopova, M. V., Karginov, V. A., Mertvetsov, N. P. & Gitelson, J. I. (1988). *Nucleic Acids Res.* **16**, 9855.

Imai, K. (1981). *IFO Res. Commun.* **10**, 64.

Jones, T. A. (1978). *J. Appl. Cryst.* **11**, 268–272.

Kabsch, W. & Sander, C. (1983). *Biopolymers*, **22**, 2577–2637.

Kasai, S. (1994). *J. Biochem.* **115**, 670–674.

Kasai, S., Fujii, S., Miura, R., Odani, S., Nakaya, T. & Matusui, K. (1991). *Flavins and Flavoproteins*, edited by B. Curti, S. Ronchi & G. Zanetti, pp. 285–288. Berlin/New York: Walter de Gruyter.

Kasai, S., Matsui, K. & Nakamura, T. (1987). *Flavins and Flavoproteins*, edited by D. E. Edmondson & D. B. McCormick, pp. 647–650. Berlin/New York: Walter de Gruyter.

Kita, A., Kasai, N., Kasai, S., Nakaya, T. & Miki, K. (1991). *J. Biochem.* **110**, 748–750.

Kita, A., Kasai, S. & Miki, K. (1995). *J. Biochem.* **117**, 575–578.

Kraulis, P. J. (1991). *J. Appl. Cryst.* **24**, 946–950.

Luzzati, V. (1952). *Acta Cryst.* **5**, 802–810.

Mancini, J. A., Boylan, M., Soly, R. R., Graham, A. F. & Meighen, E. A. (1988). *J. Biol. Chem.* **263**, 14308–14314.

Matthews, B. W. (1968). *J. Mol. Biol.* **33**, 491–497.

Meighen, E. A. (1991). *Microbiol. Rev.* pp. 123–142.

Miyahara, J., Takahashi, K., Amemiya, Y., Kamiya, N. & Satow, Y. (1986). *Nucl. Instrum. Methods A*, **246**, 572–578.

Moore, S. A., James, M. N. G., O'Kane, D. J. & Lee, J. (1992). *J. Mol. Biol.* **224**, 523–526.

Moore, S. A., James, M. N. G., O'Kane, D. J. & Lee, J. (1993). *EMBO J.* **12**, 1767–1774.

Pähler, A. & Hendrickson, W. A. (1990). *J. Appl. Cryst.* **23**, 218–221.

Raibekas, A. A. (1991). *J. Biolumin. Chemilumin.* **6**, 169–176.

Rossmann, M. G. & Blow, D. M. (1962). *Acta Cryst.* **15**, 24–31.

Sakabe, N. (1991). *Nucl. Instrum. Methods A*, **303**, 448–463.

Sambrook, J., Fritsch, E. F. & Maniatis, T. (1989). *Molecular Cloning: A Laboratory Manual*, Vols. 1–3. Cold Spring Harbor Laboratory Press.

Smith, W. W., Pattridge, K. A., Ludwig, M. L., Petsko, G. A., Tsernoglou, D., Tanaka, M. & Yasunobu, K. T. (1983). *J. Mol. Biol.* **165**, 737–755.

Soly, R. R., Mancini, J. A., Ferri, S. R., Boylan, M. & Meighen, E. A. (1988). *Biochem. Biophys. Res. Commun.* **155**, 351–358.

Soly, R. R. & Meighen, E. A. (1991). *J. Mol. Biol.* **219**, 69–77.

Steigemann, W. (1992). *PROTEIN Version* 3.1, *A Program System for the Crystal Structure Analysis of Proteins.* Max-Planck Institute für Biochemie, Martinsried, Germany.

Watenpaugh, K. D., Sieker, L. C. & Jensen, L. H. (1973). *Proc. Natl Acad. Sci. USA*, **70**, 3857–3860.